ISSN 1990-3413, Astrophysical Bulletin, 2008, Vol. 63, No. 3, pp. 228–243. © Pleiades Publishing, Ltd., 2008.
Original Russian Text © E. Sonbas, A.S. Moskvitin, T.A. Fatkhullin, V.V. Sokolov, A. Castro-Tirado, A. De Ugarte Postigo, G. Gorosabel, S. Guzij, M. Jelinec, T.N. Sokolova, V.N. Chernenkov, 2008, published in Astrofizicheskij Byulleten, 2008, Vol. 63, No. 3, pp. 244–259.

STELLAR-WIND ENVELOPE AROUND THE MASSIVE SUPERNOVA PROGENITOR XRF/GRB 060218/SN 2006aj

E. Sonbas[1,2], A.S. Moskvitin[1], T.A. Fatkhullin[1], V. V. Sokolov[1], A. Castro-Tirado[3], A. De Ugarte Postigo[3], G. Gorosabel[3], S. Guzij[3], M. Jelinec[3], T.N. Sokolova[1], and V.N. Chernenkov[1]

[1]*Special Astrophysical Observatory, Russian Academy of Sciences, Nizhnij Arkhyz, 369167 Russia*
[2]*University of Cukurova, Department of Physics, 01330 Adana, Turkey*
[3]*Instituto de Astrofisica de Andalucia (IAA-CSIC), P.O. Box 03004, 18080 Granada, Spain*

Received November 29, 2007; in final form, February 25, 2008

Abstract—The spectra of the supernova SN 2006aj identified with the X-ray flash (XRF) and gamma-ray burst XRF/GRB 060218/SN 2006aj taken with the 6-m telescope of the Special Astrophysical Observatory of the Russian Academy of Sciences are found to exhibit features, which can be interpreted as hydrogen lines. Such features indicate the existence of a stellar-wind envelope around the massive star—the progenitor of the gamma-ray burst. The results of our modeling of two early spectra taken with the 6-m telescope 2.55 and 3.55 days after the explosion of the type-Ic supernova SN 2006aj (z=0.0331) are reported. The spectra are modeled in the Sobolev approximation using SYNOW code [1, 2]. The spectra of the optical afterglow of the X-ray flash XRF/GRB 060218 are found to exhibit spectral features, which can be interpreted as: (1) the P Cyg-profile of the Hα line for the velocity of 33000 km/s—a broad and small deformation of the continuum in the wavelength interval 5600–6600Å for the first epoch (2.55 days) and (2) a part of the P Cyg-profile of the Hα line in absorption blueshifted by 24000 km/s—a broad spectral feature with a minimum at 6100Å (rest wavelength) for the second epoch (3.55 days). Given earlier observations made with the 6-m telescope and the spectra taken with other telescopes (ESO Lick, ESO VLT and NOT) prior to February 23, 2006, it can be concluded that we are observing the evolution of optical spectra of the type Ic massive supernova SN 2006aj during its transition from the short phase with the "shock breakout" into the external layers of the stellar-wind envelope to the spectra of the phase of rising supernova luminosity, which corresponds to radiative heating. We are the first to observe the signs of hydrogen in the spectra of a gamma-ray afterglow.

PACS numbers : 97.60.Bw, 98.70.Qy, 98.70.Rz
DOI: 10.1134/S1990341308030036

1. INTRODUCTION

On February 18.149, 2006 (hereafter the dates given in such a (decimal) format) Swift space observatory recorded a peculiar gamma-ray burst (GRB) accompanied by a powerful component of the radiation of a supernova (SN) in the spectra and in the light curve of the GRB afterglow. That is why this burst has been classified both as GRB 060218 and SN 2006aj: GRB 060218/SN 2006aj. However, in this case the spectrum of the GRB was dominated by X-ray radiation and therefore the gamma-ray burst was also classified as an XRF (X-Ray Flash) and the entire event is referred to as XRF/GRB 060218/SN 2006aj or XRF 060218/SN 2006aj. We use the latter designation most often to emphasize the fact that in case of SN 2006aj the supernova event began with a powerful X-ray flash.

This XRF/GRB was the first event with direct observational evidence available for the early phase of the expansion of the shock, developed as a result of the explosion of the compact core of the supernova, and the breakout of this shock toward the outer boundary of the stellar-wind envelope of the supernova progenitor. The shock was first observed (during the first two hours) in the form of the X-ray flash XRF 060218. After that, when the envelope became optically thin, the shock took the form of a powerful ultraviolet flash with maximum at the 11 hours after the detection of the GRB [3, 4]. During the first 2800 seconds the X-ray spectrum of XRF 060218 exhibited, in addition to the nonthermal emission typical to the afterglows of GRBs, a power-

ful thermal component with decreasing temperature and the maximum of emission gradually shifts into the UV–optical part of the spectrum (see Fig. 1 in the paper by Campana et al. [4] and Fig. 2 in the paper by Blustin [3]).

XRF/GRB 060218 is one of the nearest gamma-ray bursts with a redshift of z=0.0331. In this respect, it can be compared with GRB 030329/SN 2003dh, which is also identified with a type Ic SN with redshift z=0.1683. Both these events came to the focus an attention, because such coincidences (GRB and SN) are by no means common—they occur once it two—three years [5]. The study of GRB can be said to constitute a new phase of the study of the same massive SN, but from the start of the event. Therefore in such cases early spectroscopic observations are of great importance for understanding the mechanism of the explosion of both the massive SN itself and the mechanism of the formation of the source of gamma-ray bursts. The large collecting area of the 6-m telescope (BTA) of the Special Astrophysical Observatory of the Russian Academy of Sciences and its Eastern location compared to other major European observatories may become of great importance in the international program of spectroscopic observations (monitoring) of the rapidly decaying optical afterglows of gamma-rat bursts.

In this paper we report the spectra (see Fig. 1) taken with the 6-m telescope [6]. Like in case of GRB 030329/SN 2003dh [7], the spectra of XRF 060218/SN 2006aj are among the earliest spectra taken with a high signal-to-noise ratio. Table 1 lists the data on quality spectra. The high quality of the spectra allows the methods of interpretation to be used that are commonly applied to the spectra of SN Ic [1, 2].

Campana et al. [4] showed that the X-ray flash itself, the UV flash that occurred about 10–11 hours after XRF 060218 and the UV excess in the early spectra of the afterglow can be explained by the interaction of the shock from the supernova with the stellar-wind envelope around the massive progenitor star. This is the so-called "shock breakout" effect—the breakout of the shock through the envelope that surrounds the collapsing core of the star.

This effect has been long known for massive SNe (core-collapse SNe Ib/c and SNe II) [12–14] and it can be observed as a relatively short phase of the SN explosion, which begins with an X-ray flash (XRF) and ends with a bright UV flash, indicating that the shock has reached the surface of the exploding star. This process can also be viewed as the shock reaching the outer layers or the optically thin "surface" of the stellar-wind envelope that surrounds the collapsing core of SNe Ib and Ic. In cases of both the famous SN 1993J and SN 1987A as well as in case of XRF 060218/SN 2006aj this effect was observed as the early abrupt and short peak on the optical light curve—see Fig. 2 in [4] and Fig. 2 in this paper. We already mentioned this effect while explaining the very first afterglow spectra of GRB 030329/SN 2003dh taken 10 hours after GRB 030329 [7]. In case of XRF 060218/SN 2006aj the detection of the GRB at the beginning of the SN explosion, i.e., before the shock breakout, allowed its motion in the interior of the stellar-wind envelope to be observed during the first two hours as an X-ray flash with a thermal spectrum.

It is evident from Table 1 that the spectra taken with the 6-m telescope correspond to the light-curve minimum, i.e., we observe the transition:

- from phase (1) of thermal radiation associated with shock breakout to the "surface" of the stellar-wind envelope—the first peak in Fig. 2,
- to phase (2) of the subsequent rise of the SN flux with a maximum after 10 days (Fig. 2), which corresponds to (nonthermal) radiative heating of the expanding envelope of the SN resulting from the ^{56}Ni→^{56}Co→^{56}Fe decay.

Thus the physical conditions during our observations varied rapidly and our paper is dedicated to interpreting the spectra of the transition phase. However, before we start to compare the observed and theoretical spectra in the second section, we give in this section the estimates of the characteristic energies, temperatures, sizes, and velocities, which directly follow from the results of X-ray and UV observations of the XRF 060218 flash made before the beginning of the spectroscopic observations with the 6-m telescope.

1) *The Energies of the X-Ray and UV Flashes.* Campana et al. [4] report the light curves in the XRT (0.3–10 keV) and UVOT energy intervals. The same authors estimated the energy radiated via gamma and X-rays during the first two hours, when the shock breaks out through the wind. The X-ray flash energy released in this process is of the order 6×10^{49} erg. During the next 8–11 hours the UV light curve shows a powerful peak—the first maximum in Fig. 2, which is associated with the shock breakout to the surface, or, more precisely, to the outer boundary of the stellar-wind envelope, which becomes sufficiently transparent. The UV flash is actually what is called the Colgate "shock breakout" [12]. The data reported by Campana et al. [4] imply an estimate of 3×10^{49}erg for the energy released during about 28 hours in this

Table 1. Early spectra of the supernova XRF 060218/SN 2006aj taken prior to February 23, 2006 with different telescopes. We indicate the time when the spectrum was taken after the XRF/GRB 060218 flash. Here T_{sp} is the number of days elapsed since February 18.149, 2006. We list only the spectra with high signal-to-noise ratio. The table does not include the early spectra taken by Modjaz et al. [8] with the FLWO 1.5-m telescope 3.97 days after the burst due to low signal-to-noise ratio.

Telescope	T_{sp} (date in 2006)	References
MDM (2.4 m)	1.95 days (February 20.097)	[9]
BTA (6 m)	2.55 days (February 20.70)	[6]
ESO VLT (8 m)	2.89 days (February 21.041)	[10]
BTA (6 m)	3.55 days (February 21.70)	[6]
NOT (2.56 m)	3.78 days (February 21.93)	[11]

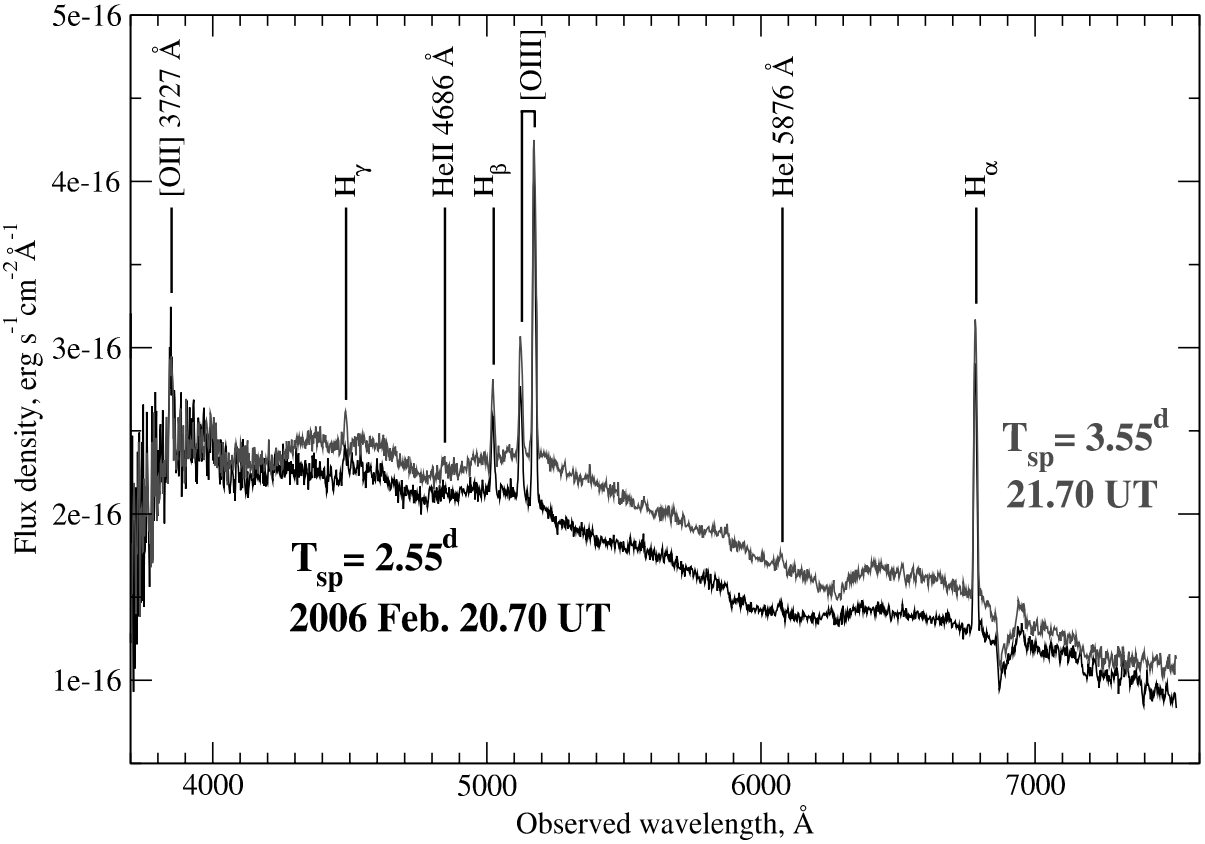

Fig. 1. Observed spectra of the afterglow of XRF 060218/SN 2006aj taken with the 6-m telescope [6]. The UT times and the time elapsed since the start of observations after the SN explosion are indicated. Also shown are the emission lines of the host galaxy (z=0.0331).

UV flash within the Swift/UVOT energy interval, thereby providing direct evidence suggesting that the X-ray and UV flash are of the same nature.

2) *Evolution of temperature.* At first, when the shock breaks through the wind envelope and energy is released mostly in X-ray interval, the thermal spectrum corresponds fairly well to temperatures of kT ≈ 0.17 keV, which are equivalent to

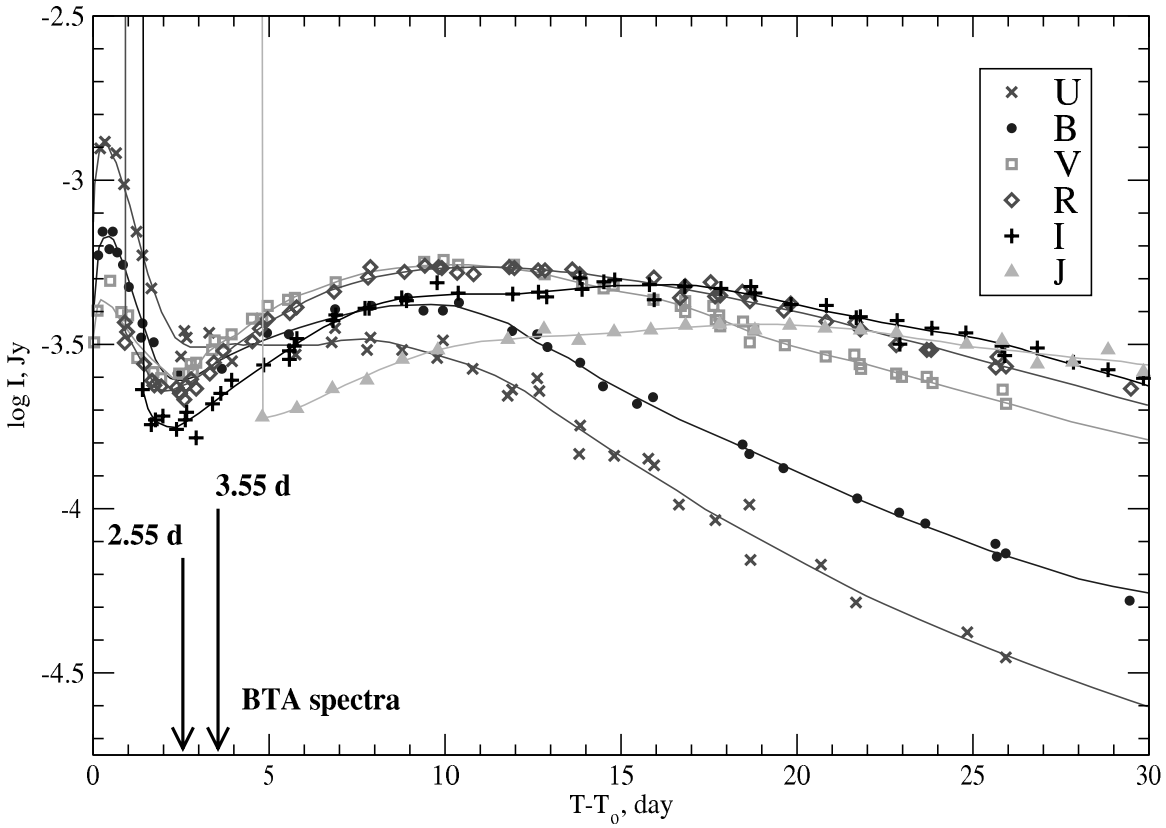

Fig. 2. Optical (U, B, V, R, I) and infrared (J) light curves of XRF 060218/SN 2006aj [15]. The first maximum corresponds to the UV flash—the shock breakout (see text). The spectra from Table 1 refer to the transition region in the vicinity if the minimum of the light curve. The arrows indicate the times when the spectra were taken with the 6-m telescope after the beginning of the SN explosion. T_0(days) corresponds to February 18.149, 2006.

2×10^6 K. By the time of the UV flash (11 hours after the GRB)—the first maximum in Fig. 2—the temperature decreases down to (0.03–0.05) keV (350 – 580 thousand K) or even lower given the uncertainties of kT measurements made by Swift/UVOT at that time (the UVOT energy interval covers only a part of the blackbody flux, see [3]). After the next 22.5 hours the temperature of the thermal component decreases down to 43000 K or to $kT \approx 3.7^{+1.9}_{-0.9}$eV ([4], Fig. 3). This leads us to suspect that, according to the estimates of the temperature decrease reported by Campana et al. [4], the temperature may be even lower than 10000 K by the time of our first spectroscopic observations (2.55 days after the GRB, see Table 1).

3) *The size of the stellar-wind envelope.* The data reported by Campana et al. [4] can also be used to estimate the radius of the wind envelope that surrounded the Wolf–Rayet star before the explosion. Blustin [3] provides arguments in favor of a Wolf–Rayet star surrounded by a dense stellar-wind envelope as the progenitor of XRF 060218/SN 2006aj. The size of this envelope can be naturally associated with the bright UV flash observed 11 hours after the GRB. At that time the shock, which was until then observed only at X-ray energies, also begins to show up at optical wavelengths, because the layers of the wind envelope above the shock become optically thin and the shock breaks out to the "surface" (more precisely, to the upper layers) of this extended envelope associated with the progenitor star/preSN. According to Swift/UVOT data on the evolution of the temperature and radius of the thermal component of the GRB/XRF 060218 afterglow, i.e., at the temperature of $kT \sim (0.03–0.05)$ keV at the time of maximum brightness ($\sim 10^4$ s), the size of the wind envelope around the pre-SN must be equal to $300R_\odot$ for a bolometric luminosity of $(4.6 - 35.5) \times 10^{45}$ erg/s.

4) *Shock velocity.* While the shock moves inside the stellar-wind envelope, the radius corresponding to the thermal component of radiation (associated with the shock breaking out from the center) increases steadily from about $5.7R_\odot$ to $17R_\odot$, as implied by the same data of Swift/UVOT X-ray observations made before the maximum of the UV flash, as reported by Campana et al. [4]. The radius of the ther-

mal component continues to increase up to $4700R_\odot$ in 1.4 days (see Fig. 3 in Campana et al. [4]), i.e., by the time of Swift/UVOT observations made after the maximum of the UV flash. By that time the shock has already broken out to the "surface" of the stellar-wind envelope and the luminosity of the thermal component decreased (see Fig. 2). We can divide the path traversed by the shock (of the radius $3.29^{+0.94}_{-0.93} \times 10^{14}$ cm of the thermal component at kT$\approx 3.7^{+1.9}_{-0.9}$ eV) by the time (1.4 days) to estimate the expansion velocity of the photosphere associated with the shock by the time of spectroscopic observations: $(2.7 \pm 0.8) \times 10^9$ cm/s [3]. Such a velocity is typical for massive SNe and it is comparable to the widths of the lines observed in the spectrum of SN 2006aj [10].

Below we will show that an analysis of our optical spectra of XRF 060218/SN 2006aj taken 2.55 and 3.55 days after the start of the SN explosion confirm the above estimates of energies, temperatures, sizes, and velocities based on the Swift/XRT/UVOT results of observations of shock breakout. At that stage the contribution of the blackbody component of the shock radiation in these spectra remained dominant as it is indicated by strong blue excesses in our spectra (Fig. 1). However, as it is evident from the UBVR light curves (Fig. 2), the GRB afterglow becomes appreciably redder in five days, and this is due to the change of the radiation mechanism of the SN by this time, when the classical, i.e., the usually observed phase of the expansion of the SN shell begins, which has been described repeatedly in many reviews (see, e.g., [16]).

In Section 2 we describe early spectroscopic observations of the optical afterglow of XRF 060218/SN 2006aj made with the 6-m telescope of the Special Astrophysical Observatory of the Russian Academy of Sciences (SAO RAS). In Section 3 we describe modeling of the spectra using SYNOW code and discuss the spectroscopic manifestations of the wind envelope in the form of broad absorptions near the restframe wavelengths of 5800Å and 6100Å, which correspond to absorption in the Hα line.

In Section 4 we discuss the results in the following context:

- The apparent evolution of the signs of the Hα line according to the data for XRF 060218/SN 2006aj obtained with the 6-meter and other telescopes,
- The manifestations of the Colgate "shock breakout" in the light curves, spectra, sizes, and luminosities of the"common" SNe Ib/c,
- The asymmetry of the explosions of massive SNe.

Finally, in Section 5 we formulates conclusions.

2. EARLY SPECTROSCOPIC OBSERVATIONS OF THE OPTICAL AFTERGLOW OF XRF 060218/SN 2006aj MADE WITH THE 6-M TELESCOPE

The program of the special observations of the optical afterglow with the 6-m telescope included the spectroscopy of the variable object discovered by Swift/UVOT telescope and identified with the XRF 060218 event. We used the SCORPIO focal reducer mounted in the primary focus of the 6-m telescope[1)]. Observations were made in two sets: 16:31-17:18, February 20, 2006 and 16:31-17:16 February 21, 2006. As the dispersive element we used a combination of a transparent grid and a VPHG550G prism with an operating wavelength interval $3500 - 7500$Å and a resolution (FWHM) of 10Å.

We reduced our observations using standard technique, which included bias subtraction; flatfielding; wavelength calibration using the comparison spectrum of a Ne-Ar lamp; atmospheric extinction correction, and absolute flux calibration using observations of a photometric standard during every observing night. We put a bright starlike object onto the entrance slit along with the optical transient in order to reveal the possible short-term variability and perform night-to-night control of the absolute-flux calibration (see Fig. 3). We made a total of four exposures during each of nights. We found no short-term variations during our observations and therefore coadded all the four individual spectra in order to improve the signal-to-noise ratio. Figure 1 shows the averaged spectra for each of the nights and Table 1 gives the average epochs for these spectra.

We then corrected the resulting spectra (Fig. 1) for Galactic extinction (Figs. 5 and 6) in accordance with the dust distribution maps [17].

The $E(B-V)$ color excess toward the object ($\alpha_{2000} = 03^h21^m39^s.683$, $\delta_{2000} = +16^\circ52'01''.82$) is equal to 0.14. We computed the extinction in terms of the dust-screen model in accordance with the formula $F_{int}(\lambda) = F_{obs}(\lambda)10^{0.4 \cdot k(\lambda)E(B-V)}$, where $F_{int}(\lambda)$ and $F_{obs}(\lambda)$ are the emitted (unabsorbed) and observed fluxes, respectively. We adopted the Milky-Way extinction curve ($k(\lambda)$) from Cardelli et al. [18].

[1)] http://www.sao.ru/hq/lsfvo/devices/scorpio/scorpio.html

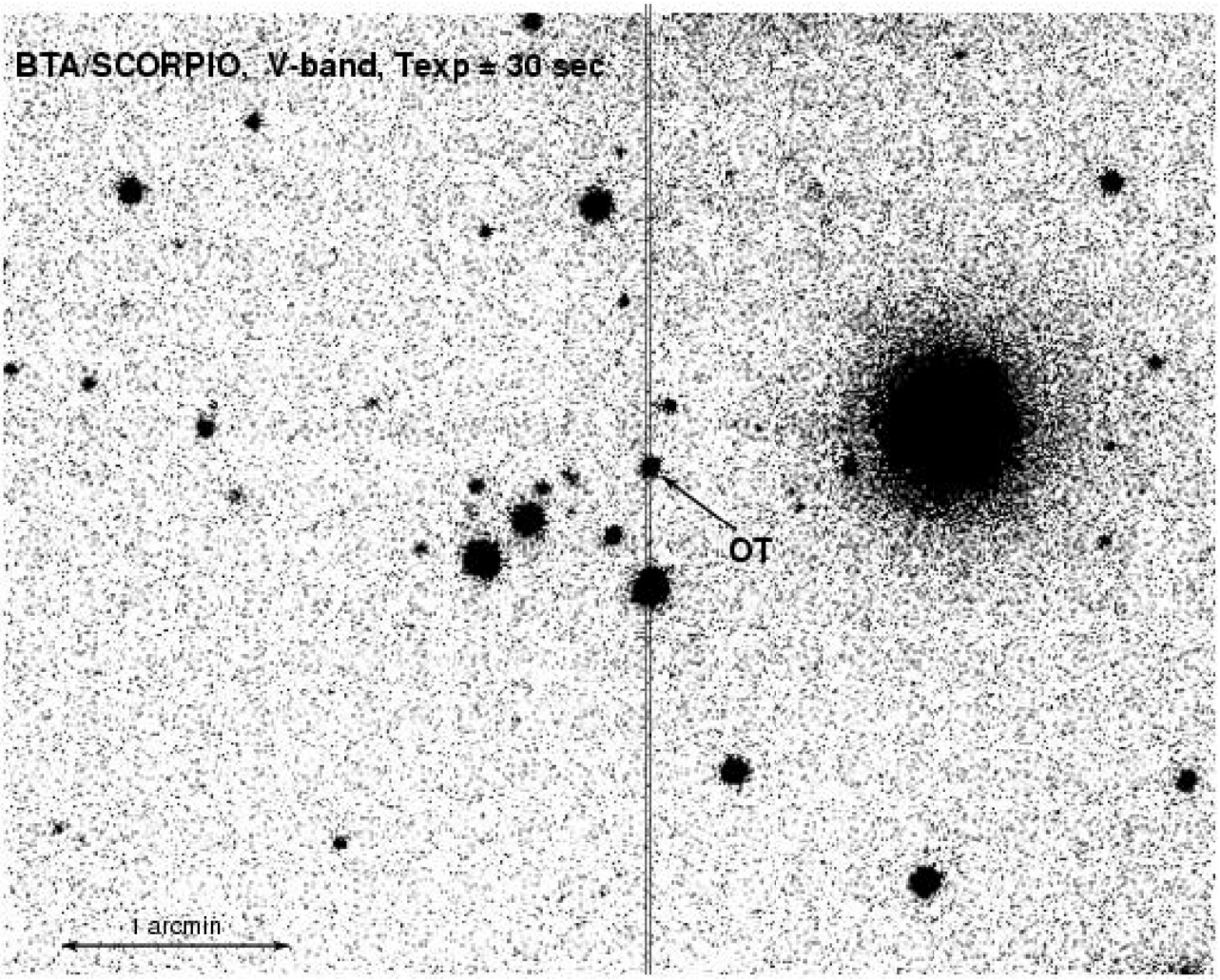

Fig. 3. Field of the optical transient. The beginning of spectroscopic observations with the 6-m telescope: February 20.647, 2006 (about 60 hours after the GRB); P.A. = 3° (the position angle of the slit); $V_{OT} = 18.16$, and $(B - R)_{OT} = 0.3$

3. COMPARISON OF THE OBSERVED SPECTRA OF XRF 060218/SN 2006aj WITH SYNTHETIC SPECTRA

To interpret the spectra obtained, we used the "SYNOW" code for computing synthetic SN spectra [1]. This multiparametric code has been used repeatedly for direct analysis of the spectra of massive SNe when hydrogen showed up at the phase of radiactive heating of the expanding envelope [2, 19, 20]. The algorithm of the computation of model spectra is based on such assumptions as: spherical symmetry; homological expansion of layers, and a sharp photospheric boundary. We can identify this optically thick photosphere, which radiates blackbody spectrum, with the shock when interpreting early spectra. This is true at least for the first days (T_{sp}=1.95 and 2.55 days from Table 1) after XRF 060218, when both the spectra (Fig. 1) and photometry (Fig. 2) exhibit strong blue excess, which is due to the blackbody radiation component from the first, short and powerful UV flash. Spectral lines are assumed to form above this expanding photosphere as a result of resonance scattering, which SYNOW codes treat in the Sobolev approximation [21–24].

This code can be used to identify the lines, estimate the expansion velocity of the photosphere and the interval of the velocities for the lines of each ion found in the spectrum. For a more detailed description of SYNOW code, see [1, 2]. To understand our results it is important that in SYNOW code the expansion velocity of the layers located above the photosphere is proportional to the distance from each point of the expanding layer to the center ($V \propto r$).

According to the shapes of the observed spectral features, the following two cases are possible: the case where the atmospheric layers where the spectral line forms does not detach from the expanding photosphere ("undetached case") and the case where these

layers detach from the expanding photosphere ("detached case"). If the matter of the moving gaseous layers located above the photosphere does not detach from the photosphere (i.e., all layers starting from the photospheric level radiate and block the photosphere) then the line is observed both in absorption and emission like in case of the classical P Cyg-type line considered in this paper (Fig. 4). We choose this model where layers do not detach from the photosphere to interpret our first spectrum (T_{sp}=2.55 days, see Fig. 1). Moreover, at this time the expanding photosphere still can be identified with the shock, because our first spectrum (with greater excess in its blue part) was taken closer to the time of the shock breakout to the "surface" of the stellar-wind envelope, which surrounded the pre-SN—the first maximum in Fig. 2.

A layer that has been detached from the photosphere shows up in the spectrum as a smoothed emission feature and a strongly blueshifted absorption—the "remnant" of the P Cyg-profile—like it is shown in Fig. 4. The atmosphere detaches when the velocity of the layer where the spectral line forms exceeds appreciably the velocity of the photosphere. If $V \propto r$ then the absorption part of the P Cyg-profile is a result of the shielding of the photosphere by a narrow layer, and the emission feature is weaker with decreasing of the thickness of the layer that emits the line. Such a model corresponds to our second spectrum (T_{sp}=3.55 days), at least for HI lines, which may form in the wind envelope. It is safe to assume that the shock has set into motion and "detached" the uppermost layers of this extended wind envelope that surounded the progenitor star of the GRB/SN.

At this phase, 3.55 days after the SN explosion, when the effect of the blackbody component becomes weaker (Fig. 2) and the expanding envelope of the SN becomes increasingly more transparent, the shock cannot be fully identified with the photosphere. At this time the so-called photospheric phase of the SN explosion begins and its spectra were the prime object for SYNOW code to interpret (see [2] and references therein).

Figures 5 and 6 compare the spectra of XRF 060218/SN 2006aj taken with the 6-m telescope 2.55 and 3.55 days after the flash with the synthetic spectra modeled using SYNOW code. The first spectrum taken immediately after the bright UV flash (Fig. 2) can be easily modeled with a rather simple set of parameters. We set the temperature of the photosphere (t_{bb}) used to fit the spectral energy distribution in Fig. 5 (with restframe wavelengths) equal to 9000 K. This also agrees with the temperature decrease rate according to the results of Swift/XRT/UVOT observations [4]; according to them the temperature must have been lower than 10000 K by the beginning of our spectroscopic observations. The SYNOW model for the spectrum taken 2.55 days after the flash implies the velocity of the photosphere to be 33000 km/s. This parameter also lies within the quoted errors of the expansion velocity of the photosphere associated with the shock estimated using the same Swift/XRT/UVOT data ($(2.7 \pm 0.8) \times 10^4$ km/s).

This means that by the beginning of our spectroscopic observations, about one day after the last Swift/UVOT observations of the decaying UV flash the shock propagation velocity remained within the same limits. Moreover, the broad and therefore barely visible depression in the continuum (see Fig. 1 with observed wavelengths) at 5900–6300Å, and the barely visible flux excess in the wavelength interval 6300–6900Å can be best fitted by a broad P Cyg-profile of the Hα line (see Fig. 5) with the same velocity of 33000 km/s. In the SYNOW code this corresponds to the undetached atmosphere case (Fig. 4.)

It is safe to assume that at this time a part of the stellar-wind envelope located above the photosphere, on an extended layer above it, move together with the photosphere and we observe the acceleration or breakout of the upper layers of this envelope. This is yet another result of the shock breakout at the "surface" of the massive circumstellar envelope that is (almost) unmoving before the SN explosion. According to the estimates given in the "Introduction", this envelope had the size of about 300 $R_\odot$, at least at the time of the shock breakout (11 hours after the GRB). To demonstrate that the barely visible flux variations in Fig. 1 in the wavelength interval 5900–6900Å of the observed spectrum can indeed be a very broad P Cyg-profile of the Hα line for velocities of about 0.3×10^{10} cm/s, we show in Fig. 5 a model spectrum with a classical P Cyg-profile, but for a much lower velocity, equal to 8000 km/s (the laboratory wavelength of the Hα is marked by a narrow emission of the host galaxy).

We fitted the undetached case to various synthetic spectra, but the velocity of the photosphere (V_{phot}) is the same for all elements and their ions (vmine) and it is equal to 33000 km/s. The main computation parameters are listed in Table 2 for the "undetached case" in Fig. 5. The only difference is in the effective formation depths of ion lines (τ/tau1), which can be chosen relatively small ($\tau < 0.5$) for all elements and ions to satisfactorily describe the observed spectrum. In the wavelength interval of about 4500–7200Å we find hydrogen to have the highest τ=0.2, whereas the other elements and their ions in synthetic spectra are taken into account even at lower τ, and this fact

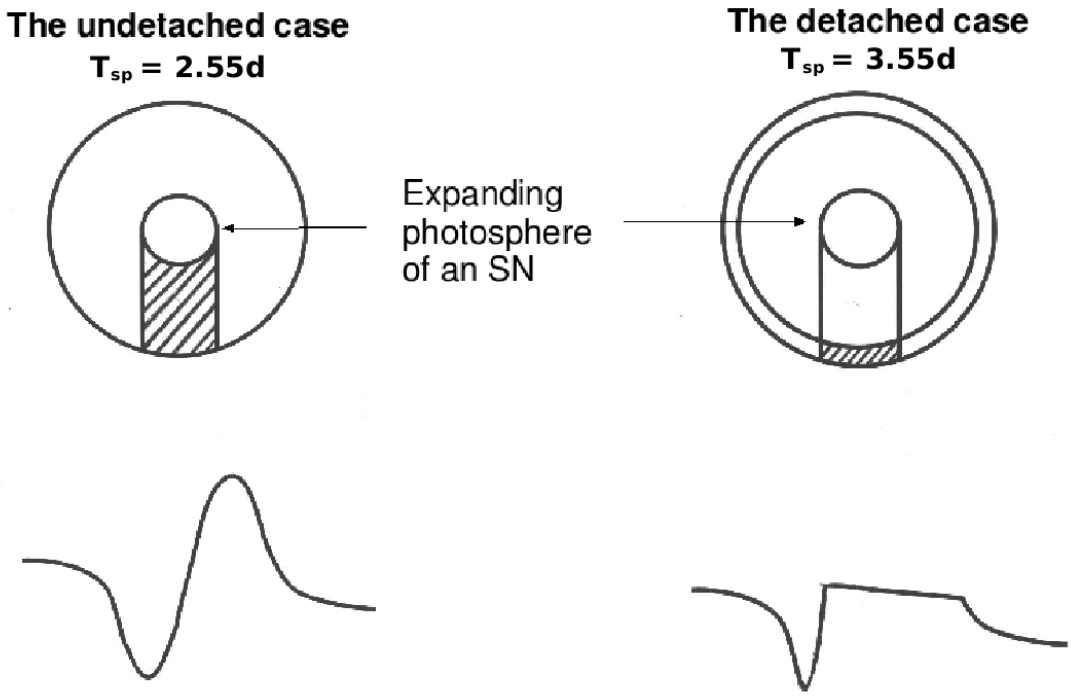

Fig. 4. The line profiles corresponding to the cases of the envelope layers undetached from the expanding photosphere and the layers detached from the photosphere (i.e., those located above the photosphere) when the gas expansion velocity increases proportionally to the distance from the center ($V \propto r$, see text). The hatched regions are those that form the absorption component of the P Cyg-profile.

may be indicative of small changes in the relative abundances of other elements compared to that of the most abundant element. This may be due to the fact that the contribution of the stellar-wind envelope remains dominant in the first spectrum (T_{sp}=2.55 days).

Note that we achieved the best agreement between the observed and synthetic spectra in the part of the spectrum where observations have the highest signal-to-noise ratio and the theoretical spectrum passes within the noise band or as close to it as possible. In particular, the slight flux deficit left of the emission line of the host galaxy [OII]3727Å (in Fig. 5) can be described by the effect of CaII with τ=0.5—it is the greatest formation depth that we use in this paper.

Our second spectrum for T_{sp}=3.55 days (see Fig. 1 with observed wavelengths) shows an absorption at 6300Å, which we interpret as a strongly blueshifted "remnant" of the P Cyg-profile of the Hα line. The best fit of the synthetic spectrum to the observed spectrum corresponds to the "detached case" in Fig. 4, where a part of the stellar-wind envelope has already "detached" from the photosphere. That is the contribution of the thermal flash (Fig. 2) rapidly decreases, the shock becomes increasingly more transparent—this is the beginning of the photospheric phase of the expansion of the SN envelope [1].

We modeled this second spectrum in the velocity interval (18000 <V< 24000) km/s (see Fig. 6 with the restframe wavelengths). The closest to the observed spectrum is the synthetic spectrum with the model parameters from Table 3, where the velocity and temperature of the photosphere are equal to 18000 km/s and t_{bb} = 8200 K, respectively. The synthetic spectrum allows for the contribution of lines with small τ(< 0.3) for the ions HI, HeI, FeII, SiII, OI, CaI, CaII, TiII, NI, CI, CII, MgI, MgII, and NaI. In Fig. 6 we presented the positions of some of these lines or the regions in the spectrum where the ion considered contributes significantly to the spectrum in case of the adopted model parameters from Table 3. The list of the reference lines used in the SYNOW code can be found in [2], and a more detailed information can be found in the SYNOW code itself [2)].

The broad absorption in the region of 6100Å (Fig. 6) can be described by the effect of HI for the "detached case" (Fig. 4) at τ = 0.16. The synthetic spectrum in this wavelength interval (5700 – 6500Å in Fig. 6) is characterized by a smoothed

[2)] http://www.nhn.ou.edu/∼parrent/synow.html

redshifted emission and a strongly blueshifted absorption with a minimum in the vicinity of 6100Å—the "remnant" of the P Cyg-profile of the Hα line.

Thus at T_{sp}=3.55 days hydrogen has already detached from the photosphere and the corresponding layer moves at a velocity of 24000 km/s (see Table 3).Here we also included all ions with small $\tau < 0.3$, but the observed spectrum cannot be described with the same values for all other parameters as it was the case in Table 2 (the "undetached case"). The layers, where most the lines of other elements form, move either with the same velocities as the photosphere (18000 km/s; OI, CaI, CaII, TiII, NI, and NaI lines), or with the same velocity as hydrogen (24000 km/s; HI, HeI, FeII, SiII, CI, CII, MgI, and MgII lines). The characteristic velocities (parameter *ve* in Table 3), which determine the characteristic thickness of the layers occupied by each element, also have to be chosen differently for different elements in order to describe best the observed spectrum. It is safe to assume that this spectrum is more affected by the chemical composition of the expanding envelope of the SN—this chemical composition has changed as a result of the evolution and explosion of the highly evolved massive core of the progenitor star.

4. RESULTS AND DISCUSSION

4.1. Evolution of the Spectra of XRF 060218/SN 2006aj and other Massive SNe

The broad and low-contrast feature in the spectrum of the afterglow of XRF060218/SN 2006aj with a minimum at the restframe wavelength of 6100Å (at z=0) can be seen in all early spectra—both our data and the spectra taken with other telescopes since February 21.70, 2006 (see Table 1). The closest one in time (February 21.93) to our second spectrum from Table 1 is the spectrum taken with the NOT telescope (see Fig. 2 in [11]), which also exhibits a minimum at the same wavelength near 6100Å. The same feature can also be seen in the ESO Lick spectrum taken on February 22.159, however, the signal-to-noise of this spectrum is appreciably lower (it is the second spectrum in Fig. 1 in [25]) than those of the two spectra mentioned above. According to the data shown in Fig. 1 of Mazzali et al [25], the feature evidently evolves beginning with the very first VLT spectrum and becomes deeper in the spectrum taken on VLT on February 23.026, i.e., about five days after XRF 060218. Mazzali et al. [25] point out that later spectra taken after the minimum on the light curve (see our Fig. 2) exhibit increasingly strong effect of the ever stronger broad absorption associated with SiII and located near 6000Å. However, the narrow minimum at 6100Å can be seen even on the VLT spectra taken in March. This is similar to what can also be seen in the spectra of some SNe Ib [26], where the narrow absorption associated with Hα also shows up and evolves in the spectra taken at the beginning of a long rise toward the brightness maximum typical to SNe Ib and Ic and similar to the rise shown in our Fig. 2.

Our spectra mentioned above also confirm the beginning of the evolution of the spectral feature at 6100Å, which can then be seen for XRF 060218/SN 2006aj according to the data obtained with other telescopes. However, we also believe that the first spectrum taken on February 20.70 with the 6-m telescope also shows the same feature—we thus interpret the broad and barely visible depression of the continuum in the wavelength interval 5600 – 6600Å (5800 – 6800Å—the observed wavelengths in Fig. 1 for T_{sp}=2.55 days) like the P Cyg-profile of the Hα line for the velocities of 33000 km/s. The same small deviation of the continuum can also be seen on the first VLT spectrum taken on February 21.041 (see Fig. 1 of Mazzali et al. [25]) eight hours after our first spectrum. As for the spectrum taken with MDM 14.5 hours before our spectrum (see Table 1), it also shows a weak deviation of the continuum at 5700Å, which can be seen despite the low signal-to-noise ratio [9]. In this case the same broad P Cyg-profile of the Hα line with velocities 30000 km/s may compete with the identification suggested by the authors. Thus, with all the early observations from Table 1 taken into account, we can conclude that we indeed observe the evolution of optical spectra—the transition from the phase of the Colgate "shock breakout" effect and the associated powerful (thermal) UV flash to the spectra of the phase of the SN light-curve rise, which corresponds to radioactive (nonthermal) heating resulting from the $^{56}Ni \rightarrow ^{56}Co \rightarrow ^{56}Fe$ decay.

This must be the main difference and novelty of our approach toward the interpretation of early spectra of XRF 060218/SN 2006aj compared to the approach employed by Mazzali et al. [25], who identify the VLT/Lick spectra of this SN and consider the theoretical spectra only for the phase of radioactive heating—see the light curve (Fig. 2) in [30]. Moreover, even the authors of SYNOW code [1, 2, 19, 20], who compute their synthetic spectra with signs of the Hα line when analyzing the spectra of common SNe Ib-c ("stripped-envelope SNe"), do not include a significant contribution of the thermal radiation from the UV flash at all early phases and, in the cases where such a contribution is taken into account, the corresponding computations are not performed for such high expansion velocities as those observed for XRF 060218/SN 2006aj.

Table 2. Table of the model parameters set for the computations in the case where the layers of the elements and ions are undetached from the photosphere ("the undetached case" in Fig. 4). The parameters correspond to the synthetic spectrum shown by a thick black line in Fig. 5 (see text). See `http://www.nhn.ou.edu/~parrent/synow.html` for more detailed information about setting the parameters for the SYNOW code

Parameters	"the undetached case"
V_{phot} [a]	33000
V_{max} [b]	70000
t_{bb} [c]	9000
ai [d]	HI, HeI, FeIII, FeII, SiII, SiI, OI, CaII, TiII, CII, CI, NI, MgII, MgI, MnII, NeI
tau1 [e]	0.2, 0.08, 0.04, 0.04, 0.0002, 0.0002, 0.002, 0.5, 0.02, 0.0005, 0.0005, 0.1, 0.0002, 0.0002, 0.0002, 0.0005
vmine [f]	33.00 for all ions
ve [g]	20.00 for all ions

[a] V_{phot} - velocity of the phortosphere in km/s.
[b] V_{max} - the upper limit for the velocities in the model.
[c] t_{bb} - the temperature of the photosphere in K.
[d] ai - the ionization stages of all ions included into the model.
[e] tau1 - the corresponding effective optical depths of the formation the lines of each species.
[f] vmine - the lowest velocities above the photosphere for each species (in 1000 km/s)
[g] ve - characteristic velocities (v_e) that we use in the adopted law, the dependences of the optical depths τ of the lines of the given species on v, $\tau(r) \propto \exp(-v(r)/v_e)$, where $v \propto r$.

Table 3. Parameters of the SYNOW model for the case where the layers of some elements in the expanding envelope of the SN have detached from the photosphere (the "detached case" in Fig. 4). The parameters correspond to one of the synthetic spectra shown in Fig. 6 by a thick black line (see text).

Parameters	"detached case"
V_{phot}	18000
V_{max}	75000
t_{bb}	8200
ai	HI, HeI, FeII, SiII, OI, CaI, CaII, TiII, CII, CI, NI, MgII, MgI, NaI
tau1	0.16, 0.02, 0.08, 0.03, 0.1, 0.3, 0.3, 0.02, 0.0004, 0.04, 0.100, 0.005, 0.03, 0.02
vmine	24.00, 24.00, 24.00, 24.00, 18.00, 18.00, 18.0, 18.00, 24.0, 24.0, 18.0, 24.0, 24.0, 18.00
ve	10.00, 20.00, 20.00, 20.00, 20.00, 10.00, 10.0, 20.00, 10.0, 10.0, 20.0, 20.0, 20.0, 20.00

Mazzali et al. [25] modeled the evolution of all the 16 ESO Lick and ESO VLT spectra of SN 2006aj [10] up to March 10, 2006 (20 days after XRF 020618) using Monte-Carlo method and a refined program of the synthesis of SN spectra based on the same assumptions as SYNOW code, but with the account taken of the model distributions of density and temperature in the envelope above the photosphere, radiative transfer with line transitions and electron scattering (see [27–29] for the details of the method).

All the characteristic features of SNe Ic become increasingly stronger in the spectra before the broad maximum on the light curves of SN 2006aj (about 10 days after the GRB in Fig. 2) and after this maximum. The spectra are modeled for the velocity interval ($20000 < V < 30000$) km/s. The strongest features

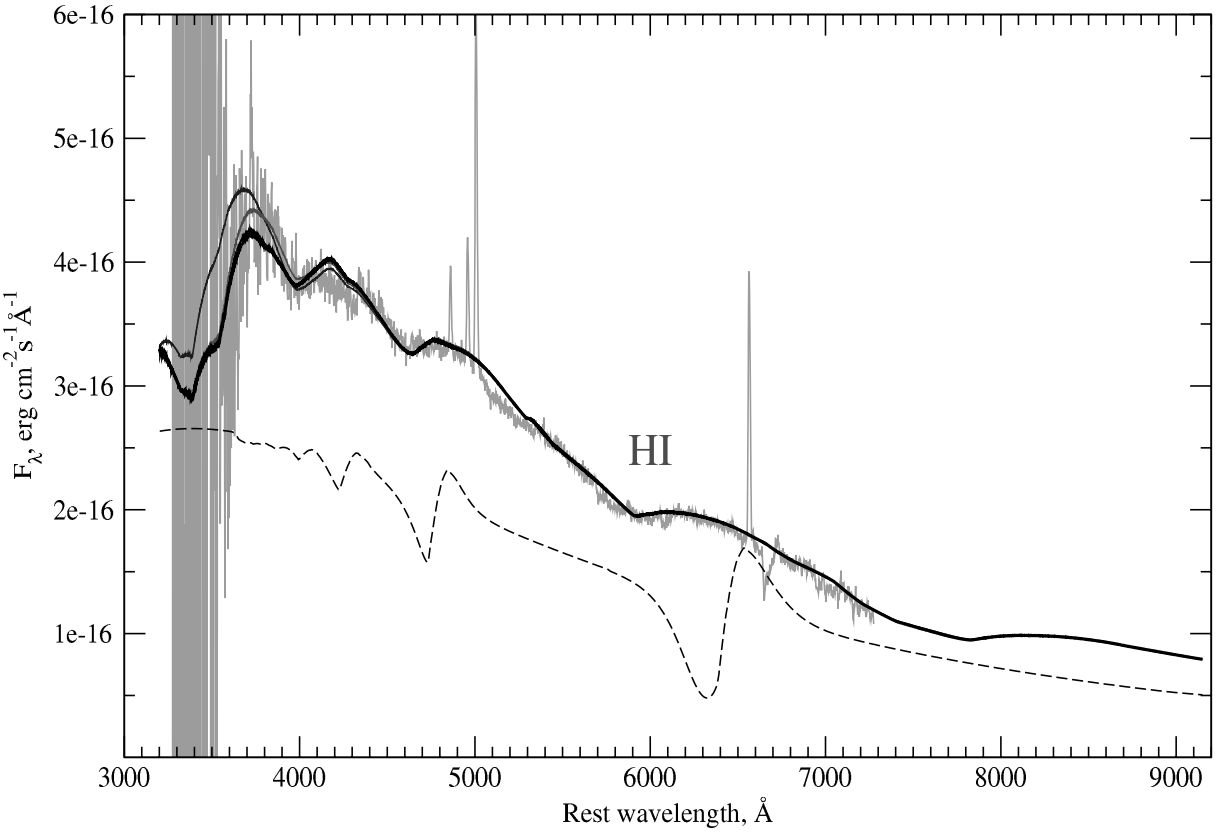

Fig. 5. The restframe (z=0) spectrum of the afterglow of XRF/GRB060218/SN 2006aj taken with the 6-m telescope 2.55 days after the explosion and corrected for Galactic extinction. Shown is its fit for the "undetached case" by synthetic spectra with the velocity of the photosphere (V_{phot}) equal to to 33000 km/s for all elements and their ions (vmine)—the smooth lines (they differ only in the blue part of the spectrum at λ<4000Å—see text). The main parameters for the computation of the synthetic spectrum shown by the thick black line are listed in Table 2. Here HI indicates the P Cyg-profile of the Hα line at V_{phot} = 33000 km/s. As an example of the Hα P Cyg-profile the dashed line shows the model spectrum for the velocity of the photosphere equal to 8000 km/s.

in the spectra mentioned by the above authors are FeII, TiII, and (at later stages) CaII (< 4500Å), FeIII and FeII (near 5000Å), SiII (near 6000Å), OI (near 7500Å), and CaII (near 8000Å).

We take all this list into account while interpreting our early spectra using SYNOW code (see Fig. 6) in almost the same velocity interval. However, we also include the contributions from the HI and HeI lines. It is evident from the computations of Mazzali et al. [25] that the above authors did not take into account the evident signs of the Hα line for the earliest spectra taken on February 21, 22, and 23 and later spectra take into account only the increasingly stronger effect of SiII near 6000Å—see Fig. 1 of Mazzali et al. [25]. At the same time, we pointed out above that the absorption feature with a minimum at 6100Å can be traced in the observed spectra at least up to March 4. It is the most conspicuous feature near 6000Å in the early spectrum taken on February 23 throughout the entire wavelength interval from 5000Å to 8500Å, where the Monte-Carlo method reveals no absorption at 6100Å.

4.2. Hydrogen Signatures in the Spectra of Massive SNe

Hydrogen signatures are by no means uncommon in the spectra of SNe Ib and Ic (Ib-c). In particular the SYNOW code mentioned above revealed the signs of hydrogen and evolution of the blueshifted Hα line when analyzing a series of optical spectra for common massive SNe Ic and Ib. Note that in this analysis special attention was given to the traces of hydrogen in observations of such stripped-envelope SNe (i.e., SNe Ib-c), although, according to the formal definition of these SN types they have no evident and immediately apparent hydrogen lines in their optical spectra. SNe Ib-c are usually analyzed in terms of the model of gravitational collapse of massive and

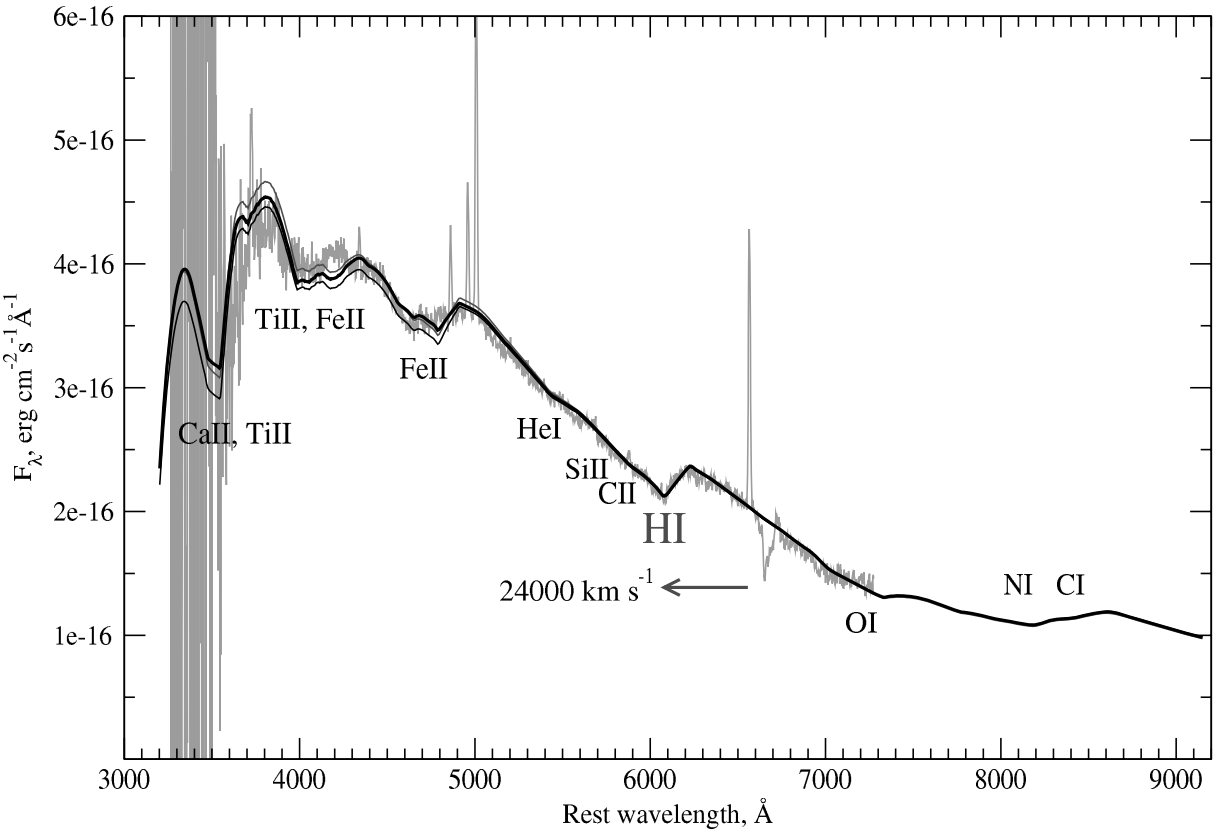

Fig. 6. The restframe (z=0) spectrum of the afterglow of SN 2006aj/XRF060218 taken with the 6-m telescope 3.55 days after the explosion and corrected for Galactic extinction. The synthetic spectra are shown by smooth lines. Shown are the positions of of the spectral lines of some ions and blends of their lines in the regions of the spectrum where the ion in question contributes significantly to the spectrum in the case of the adopted model parameters. The thick black line shows the synthetic spectrum computed with the parameters from Table 3 when the absorption at 6100Åcan be described by the dominant effect of HI for the "detached case". It is a strongly blueshifted part of the P Cyg-profile of the Hα line for the expansion velocity of the detached HI layer equal to 24000 km/s.

stripped-envelope SNE Ib-c, which have lost their envelope before the collapse; carbon-oxygen cores, and, signs of this envelope must apparently always show up in the spectra of such SNe. However, hydrogen can be more or less confidently identified only in sufficiently early spectra of SNe Ib-c, as shown by Branch et al. [19], Baron et al. [20], Branch et al. [27], Elmhamdi et al. [2], and Parrent et al. [26].

According to a possible competing hypothesis for describing the spectral feature with a minimum near 6100Å, it can be interpreted as the absorption component of the P Cyg-profile of the CII 6580Å line [27]. However, if this entire extended (about $300\,R_\odot$) stellar-wind envelope first showed up as an X-ray flash and then as an UV flash in the afterglow of XRF 060218/SN 2006aj, at least the unevolved part of the envelope, which is at the stellar-wind stage of the evolution of the massive progenitor star and formed long before the SN explosion, must be associated with neutral hydrogen. The fact that hydrogen always shows the highest velocity contrast between the filled HI layer and the photosphere compared to other elements in the spectra of SNe Ib-c also supports the hypothesis that these very layers (that are associated with the wind envelope) are the first to start moving as a result of the SN explosion: [1] (see Fig. 9), [2] (see Fig. 5), and [19] (see Fig. 23). We can also estimate the mass of this part of the envelope that has begun to move (the masses of gas in Hα or in the HI layer) using the equation from the paper by Elmhamdi et al. [2] as follows:

$$M(M_\odot) \simeq (2.38 \times 10^{-5}) v_4^3 t_d^2 \tau(H\alpha),$$

where the time after the explosion, t_d, is in days; v_4 is the velocity of the layer in the units of 10^4 km/s, and τ(Hα) is the formation depth of the line. In this equation derived for the Sobolev optical depth in the expanding envelope [2, 30] we use the velocity 24000 km/s, which refers only to the moving part of the HI layer (see the data in Table 3). It also

corresponds to the "detached case" in Fig. 4. As a result the mass of the HI layer is of the order of $6 \times 10^{-4} M\odot$, and its distance from the center by that time (3.55 days after the SN explosion) is no less than 7.36×10^{14}cm.

4.3. The Colgate "Shock-Breakout" Effect in XRF 060218/SN 2006aj and Other SNe—the Light Curves, Spectra, Luminosities, and Sizes

SNe Ib and Ic have been observed since long and their most likely progenitors are believed to be Wolf–Rayet stars surrounded by a more or less dense wind envelope , which is a result of the evolution of massive star. The shock that develops during the explosion of the evolved core of the star traverses the envelope and produces a bright and short X-ray and UV flash, which may last several hours—the duration of the flash depends on how massive and extended was the wind envelope that surrounded the progenitor star before the SN explosion. The interaction between the shock produced by the SN explosion and the envelope (the "shock breakout" effect) has been predicted long ago [12, 31, 32]. In particular, Calzavara and Matzner [14] dedicated their paper to future systematic observations of this effect. However, before the XRF 060218/SN 2006aj event the effect in question could have been fully observed only for a small number of massive SNe.

Very short—due to the compact size of the blue supergiant ($20–30 R_\odot$)—effect of the interaction of the shock was observed (albeit not from the very beginning) in the famous SN 1987A of type II (see the review by Imshennik and Nadezhin [16]). The shock interaction effect was observed over a long—two-to-three weeks—time interval in a very extended (of the order of 10^{15} cm) envelope of the type IIn supernova SN 1994W—see, e.g., [33]. In other SNe Ib-c the effect was observed only at its very end before the subsequent rise of the SN flux, which corresponds to the ^{56}Ni→^{56}Co→^{56}Fe radioactive heating—this was the case of SN 1999ex [34]. Similar "remnants" of this effect can be seen (in the R band) even for SN 1998bw, which is usually associated with GRB 980425 (see [35]).

SN 1993J in M81: One can say that SN 1993J was observed almost at the very beginning of the explosion. We say "almost", because in this case the time of the beginning of the SN explosion is known to within 12 hours and not to within several seconds as in case of the XRF/GRB SN. This SN was first classified by its spectrum as a type II SN because of hydrogen lines appear in its early spectra (Fig. 7). However, after a certain time this SN changed its type to Ib [37], when hydrogen ceased to be confidently seen in the spectra. The early spectra of SN 1993J in Fig. 7 show a strong UV excess, which is characteristic of the shock interaction, and the smoothed continuum with almost no lines beyond 5000Å, which resembles the spectrum of XRF 060218/SN 2006aj in Fig. 5, although in case of SN 2006aj the expansion velocities are significantly higher (see below the comments about the possible asymmetry of explosions of SNe identified with GRBs). SN 1993J also had an unusual light curve with the luminosity increased rapidly up to the first maximum, and then abruptly decreased during several days, and then slowly increases again over the next two weeks—a behavior similar to that shown in Fig. 2 for XRF 060218/SN 2006aj. The light curve of SN 1993J has been since long modeled by many groups [38–40]. The above authors pointed out that such a behavior of the light curve of SN 1993J can be explained by the interaction of the shock with an extended (about $300 R_\odot$) hydrogen envelope of mass $1 M_\odot$ around the progenitor star. Note that the luminosity achieved at the summit of the first (fast) maximum, which lasts only about 4–5 hours, may be as high as 10^{45} erg/s, and a full energy release of the order of 5×10^{49} erg.

It is not surprising that approximately same envelopes can also explain the flash due to shock breakout, in case of XRF/GRB 060218/SN 2006aj. In this case the total energy released by the SN is of the same order, about, 10^{49} erg. However, in case of SN 1993J there was no gamma-ray burst and everything seems to be explained by the asymmetry of the SN explosion (see below).

The fact that GRB/XRF 060218/SN 2006aj is yet another case where the Colgate effect could have been observed in pure form and since the very beginning of the SN explosion can be understood as a hint suggesting that the gamma-ray burst may be the first signal in gamma rays, which is indicative of the beginning of the collapse of the massive core, followed by the entire process—the explosion of a massive SN: the burst may be followed by an X-ray and then a powerful UV flash. In this case a search for all kinds of manifestations of wind envelopes around massive progenitor stars in early spectra and in photometry of the XRF/GRG afterglow may become the key point in optical observations of transient sources associated with XRF/GRB, because the interaction of the SN shock with these envelopes is the first optical event after the beginning of the collapse of the massive core of the star, and here we can expect manifestations of new effects associated with, e.g., the asymmetry of the explosion.

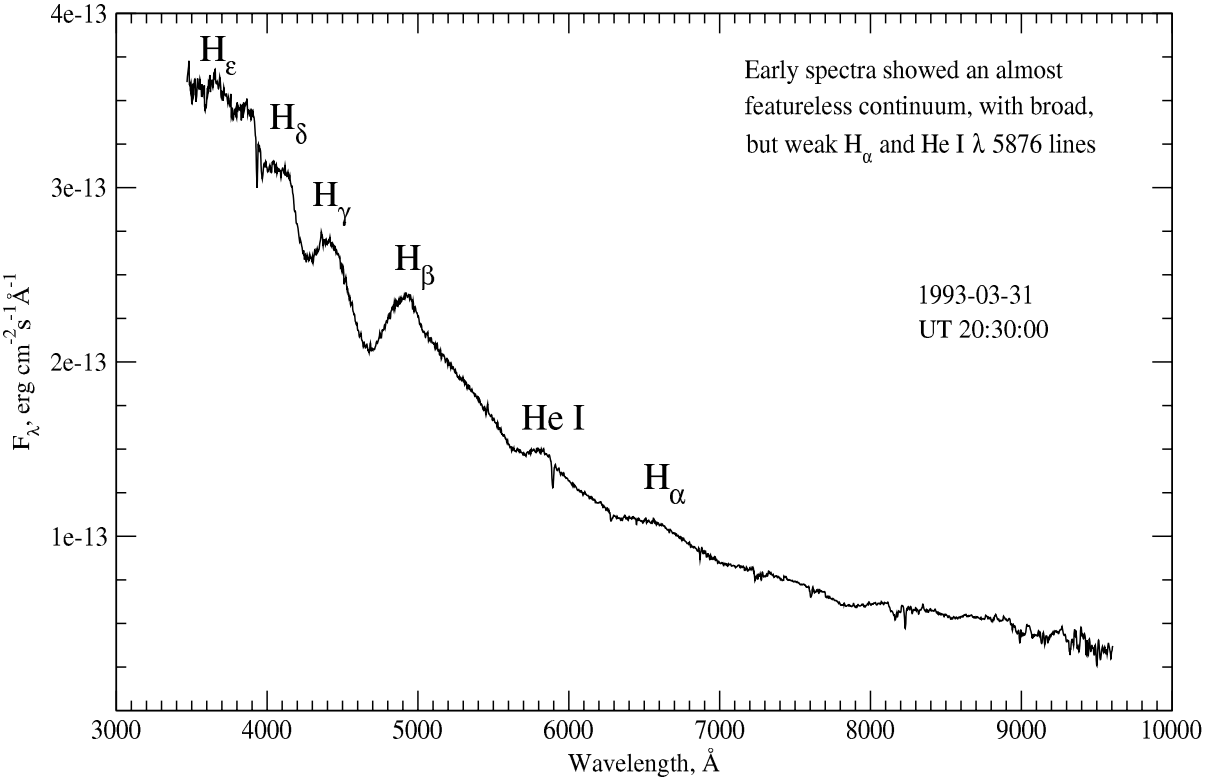

Fig. 7. The earliest optical spectrum of SN 1993J (see text). We adopted this spectrum from SUSPECT - The Online Supernova Spectrum Database `http://bruford.nhn.ou.edu/suspect/` ([36]).

4.4. Asymmetry of type Ib and Ic Supernova Explosions

The XRF 060218/SN 2006aj explosion was indeed a classical XRF event [4, 41]. The fact that in case of common and nearby SNe the explosion starts not with a gamma-ray burst can be naturally explained by the asymmetric, axisymmetric, or bipolar (with the formation of jets) explosion of massive SNe. One of the now popular hypotheses (see the references in [42]) is based on the assumption that in case of an XRF type flash the observer is located outside the cone where for some reasons the bulk of gamma-ray radiation is concentrated.

The farther is the observer from the axis of the SN explosion, the more X-ray photons and the less gamma-ray photons are recorded from the burst—GRB pass into X-ray Rich GRB (like GRB 030329) and become XRF [43]. If the SN is observed at an angle close to 90° to the explosion axis, no gamma-ray burst is observed and only an X-ray flash is seen followed by a powerful UV flash caused by the interaction of the shock with the envelope surrounding the pre-SN, as it was the case of SN 1993J.

Thus, if the SN is observed from a direction that is close to the equator of the explosion (and this is the most likely situation) and if the massive collapsing core of the star is surrounded by a sufficiently dense stellar-wind envelope then the effect considered should be observed only at X-ray and gamma-ray energies. In this case the contribution of the afterglow of the gamma-ray burst to the light curve of a "common" SN may be insignificant. One way or another, but it must be significantly smaller than in case of a classical GRB observed close to the axis of the SN explosion (the most likely situation). In this connection, Filippenko et al. [44] recently pointed out that a significantly asymmetric explosion may be a characteristic feature of massive SNe of all types, although it is still unclear whether the mechanism that generates the gamma-ray burst is responsible for the explosion of the star.

5. CONCLUSIONS

In this paper we provide additional arguments in favor of the stellar-wind origin of the shock interaction effect, which was earlier found using Swift/XRT/UVOT [4] observations of the XRF/GRB 060218 burst. In our optical spectra of the afterglow of XRF/GRB 060218 we found spectral features, which we interpret as hydrogen lines

observed in early ESO Lick, ESO VLT, and NOT spectra [10, 11]. We are the first to discover hydrogen in the spectra of an afterglow of a gamma-ray burst, which constitutes direct evidence for the afterglow of gamma-ray burst.

We present the results of our modeling of two spectra taken with the 6-m telescope 2.55 and 3.55 days after the explosion of SN 2006aj, which is associated with the X-ray flash XRF/GRB 060218. We modeled the spectra in the Sobolev approximation using SYNOW code [1, 2]. In these early spectra of SN 2006aj, which is a SN Ic, we found spectral features, which we interpreted as:

1) The P Cyg-profile of the Hα line for velocities of the order of 33000 km/s—a broad and barely visible deformation of the continuum in the interval of restframe wavelengths 5600 – 6600Å for the first epoch.

2) A part of the P Cyg profile of the Hα line in absorption blueshifted by 24000 km/s—a broad and low-contrast spectroscopic feature with a minimum at about 6100Å (rest wavelength) for the second epoch (3.55 days).

The evolution of the same spectral features can also be traced by the spectra of SN 2006aj taken with other telescopes [10, 11]. Such Hα lines may directly confirm the existence of a stellar-wind envelope, which was already observed during the XRF/GRB 060218 burst in the form of a powerful blackbody component, first at X-ray wavelengths and then in the optical spectrum [4]. Thus, given early observations made with the 6-m telescope of the Special Astrophysical Observatory of the Russian Academy of Sciences, we can conclude (Table 1) that we observe the evolution of optical spectra of the massive SN 2006aj—the transition from the phase of the Colgate effect to the phase of flux increase, which corresponds to radiative heating.

Our identification of these features with the Hα line in the early spectra of the type Ic SN 2006aj is also corroborated by spectroscopic observations of common (not identified with the GRB) massive SNe Ic and Ib, where hydrogen was found using SYNOW code [2, 19, 27].

If observations of afterglows and other bursts continue to confirm the interpretation of the thermal component in the spectrum of the GRB/XRF 060218 burst as the interaction of the SN shock with the wind envelope of the progenitor star of SN 2006aj/XRF 060218 then this fact should provide a new impetus to the development of the theory of both gamma-ray bursts themselves and massive SNe. Gamma-ray bursts and associated SNe (GRB/SN) with small z are observed (albeit relatively rarely [5], however, they are the most data-rich events, such as XRF/GRB 060218/SN 2006aj or GRB 030329/SN 2003dh) in terms of the elucidation of the relation between gamma-ray bursts and SNe. Note that the search for wind envelopes around massive gamma-ray progenitors both in early spectra and photometry of the afterflow of these GRBs, can be a key moment in the study of these transient sources.

ACKNOWLEDGMENTS

We are grateful to David Branch and other authors of SYNOW code for their consultations on running the code at the Special Astrophysical Observatory of the Russian Academy of Sciences and its practical use. We are also grateful to E. L. Chentsov and S. N. Fabrika for reading the first version of the text and constructive criticism. This paper was supported in part by the Spanish research programs ESP2005-07714-C03-03 and AYA2004-s.

REFERENCES

1. D. Branch et al., Supernovae and Gamma-Ray Bursters. Ed. by K. Weiler., Lecture Notes in Physics, **598**, 47 (2001) (astro-ph/0111573).
2. A. Elmhamdi et al., Astronom. and Astrophys. **450**, 305 (2006) (astro-ph/0512572).
3. A. J. Blustin, astro-ph/0701804.
4. S. Campana et al., Nature **442**, 1008 (2006).
5. R. Chapman, N. R. Tanvir, R. S. Priddey, and A. J. Levan, astro-ph/arXiv:0708.2106.
6. T. A. Fatkhullin et al., GCN **4809**, 1 (2006).
7. V. V. Sokolov et al., Bull. Spec. Astrophys. Obs. **56**, 5 (2003).
8. M. Modjaz et al., Astrophys. J. **645**, L21 (2006).
9. N. Mirabal et al., Astrophys. J. **643**, L99 (2006).
10. E. Pian et al., Nature **442**, 1011 (2006).
11. J. Sollerman et al., Astronom. and Astrophys. **454**, 503 (2006).
12. S. A.Colgate, Canadian Journal of Physics **46**, 476 (1968).
13. V. S. Imshennik and D. K. Nadezhin, Sov. Sci. Rev. E. Astrophys. Space Phys. **8**, 1 (1989).
14. A. J. Calzavara and C. D. Matzner, Monthly Notices Roy. Astronom. Soc. **351**, 694C (2004) (astro-ph/0312464).
15. M. Jelinek et al., 2007 (in preparation).
16. V. S. Imshennik and D. K. Nadezhin, Uspekhi Fiz. Nauk **156**, 521 (1988).
17. D. Schlegel, D. Finkbeiner, and M. Davis, Astrophys. J. **500**, 525 (1998).
18. J. A. Cardelli, G. C. Clayton, and J. S. Mathis, Astrophys. J. **345**, 245 (1989).
19. D. Branch et al., Astrophys. J. **566**, 1005 (2002).

20. E. Baron et al., ASPC **342**, 351 (2005).
21. V. V. Sobolev, *"Kurs Teoreticheskoi Astrofiziki" (A Course of Theoretical Astrophysics)*, 2007, Ch. VI, Section 28, Pt.2 [in Russian].
22. V. V. Sobolev, *Theoretical Astrophysics* (Pergamon Press Ltd., London, 1958).
23. V. V. Sobolev, *Moving Envelopes of Stars* (Harvard University Press, 1960)
24. V. G. Gorbatskii and I. N. Minin, *"Nestatsionarnye Zvezdy" (Nonstationary Stars)*, 1963, Ch. VI, Section 24 [in Russian].
25. P. A. Mazzali et al., Nature **442**, 1018 (2006).
26. Parrent et al., astro-ph/0701198.
27. D. Branch et al., astro-ph/0604047.
28. L. B. Lucy, Astronom. and Astrophys. **345**, 211 (1999).
29. P. A. Mazzali et al., Astronom. and Astrophys. **279**, 447 (1993).
30. J. I. Castor, Monthly Notices Roy. Astronom. Soc. **149**, 111 (1970).
31. G. S. Bisnovatyi-Kogan et al., Ap. Space. Sci. **35**, 23 (1975).
32. S. I. Blinnikov et al., astro-ph/0212569.
33. N. Chugai et al., astro-ph/0405369.
34. Stritzinger et al., Astrophys. J. **124**, 2100 (2002).
35. T. Galama et al., Nature **395**, 670 (1998).
36. D. Richardson et al., Astronom. and Astrophys. Suppl. Ser. **201**, 5609R (2002).
37. A. V. Filippenko, T. Matheson, and L.C. Ho, Astrophys. J. **415**, L103 (1993).
38. K. Nomoto et al., Nature **364**, 507 (1993).
39. T. R. Young et al., Astrophys. J. **449**, L51 (1995).
40. T. Shigeyama et al., Astrophys. J. **420**, 341 (1994).
41. J. Heise, in't Zand J., R. M. Kippen, and P. M. Woods, in *Proceedings of the International Workshop, Rome, Italy, 2000*, astro-ph/0111246.
42. A. Soderberg et al., astro-ph/0502553.
43. V. V. Sokolov et al., Bull. Spec. Astrophys. Obs. **59**, 5 (2006).
44. A. Filippenko et al., astro-ph/0603297.